

Supporting Information  
**Polar-Hydrophobic Ionic Liquid Induces Grain Growth and Stabilization in Halide  
Perovskites**

Dan Liu,<sup>a,b,#</sup> Zhipeng Shao,<sup>c,#</sup> Jianzhou Gui,<sup>a</sup> Min Chen,<sup>b</sup> Mingzhen Liu,<sup>d</sup> Guanglei Cui,<sup>c</sup> Shuping Pang,<sup>c</sup> Yuanyuan Zhou<sup>b\*</sup>

<sup>a</sup> State Key Laboratory of Separation Membranes and Membrane Processes, Tianjin Key laboratory of Green Technology and Process Engineering, School of Chemistry and Chemical Engineering, Tianjin Polytechnic University, Tianjin 300387, P.R. China.

<sup>b</sup> School of Engineering, Brown University, Providence, Rhode Island 02912, United States; Email: [yuanyuan\\_zhou@brown.edu](mailto:yuanyuan_zhou@brown.edu);

<sup>c</sup> Qingdao Institute of Bioenergy and Bioprocess Technology, Chinese Academy of Sciences, Qingdao 266101, P.R. China;

<sup>d</sup> School of Materials and Energy, University of Electronic Science and Technology of China, Chengdu 611731, P.R. China.

## Experimental Section

### Materials Synthesis and Film Fabrication

All raw chemicals are obtained from Sigma-Aldrich, USA with further purification except when mentioned specifically. MA<sup>+</sup>TFA<sup>-</sup> ionic liquids (ILs) are synthesized via proton transfer between a Brønsted acid, trifluoroacetic acid and a weak base, methylamine. Anhydrous trifluoroacetic acid (Sigma-Aldrich, USA) and methylamine (MA, 33 wt.% in ethanol solution; Sigma-Aldrich, USA) are reacted in the equimolar amount. Since these reactions are very exothermic, the dropwise addition of the acid to the amine was carried out by cooling the amine solution to 0 °C using an ice water bath. The mixture was then stirred at room temperature for 6 hours. To ensure a complete reaction, an excess of amine was used and then removed in vacuum using a rotary evaporator.

### Film Fabrication:

For the deposition of MAPbI<sub>3</sub> perovskite thin films with on FTO-coated glass substrates, a 40 wt% PbI<sub>2</sub>:MAI (molar ratio 1:1) mixture was dissolved in the N,N-dimethylmethanamide (DMF) solvent, with different amount of MA<sup>+</sup>TFA<sup>-</sup> as the additive, were prepared. The solutions were spin-coated on the substrates at 4000 rpm for 20 s. The as-formed thin films were then annealed at 130 °C for 10 min. For obtaining better-quality thin films, the chlorobenzene-solvent-dripping process was introduced during the spin-coating step. Typically, the weight ratios of MA<sup>+</sup>TFA<sup>-</sup> and MAPbI<sub>3</sub> are 1:35, 1:25, 1:15 and 1:10, respectively.

**Materials and Thin-Film Characterization.** Qualitative analysis of as-synthesized MA<sup>+</sup>TFA<sup>-</sup> ILs has been carried out by Fourier-transform infrared spectroscopy (FTIR;

iS50, Nicolet, Thermo Scientific, USA) and  $^1\text{H}$  NMR (Advance III HD 400, Bruker, USA). Thermogravimetry and Differential Thermal Analyses (TG-DTA) of the samples were studied via a TG analyzer (DTG-60, Shimadzu, Japan) within the temperature range of 30 to 500 °C. The measurement process was carried out in the air with a heating rate of 10 °C/min. X-ray diffraction (XRD) patterns were collected using an X-ray diffractometer (D8 Discover, Bruker, Germany) using Cu K $\alpha$  radiation ( $\lambda=1.5406$  Å) at step size of 0.02°. 2D XRD were performed on an X-ray diffractometer with an in-situ heating stage (D8 Advance, Bruker, Germany). UV-vis absorption spectra were obtained on a UV-vis spectrometer (UV-2600, Shimadzu Scientific, Japan). Photoluminescence (PL) spectroscopy was performed on a spectrometer (FluoTime 300, PicoQuant, Germany) using 405 nm laser excitation. The surface and cross-sectional morphology and microstructure of samples were observed by a scanning electron microscopy (SEM; G500, ZEISS, Germany). Energy dispersive X-ray spectrometer (EDS; Octane Elite EDS System, EDAX, USA) attached to the SEM was employed for elemental analyses. The surface chemical compositions were measured using X-ray photoelectron spectroscopy (XPS; K-alpha, Thermo Scientific, USA).

**PSC Fabrication and Testing.** Patterned FTO-glass substrates were cleaned ultrasonically with an alconox (detergent) solution, followed by sonication in deionized water, acetone, and isopropyl alcohol sequentially for 20 min each. A 30-nm compact-TiO $_2$  layer was deposited on top of the etched FTO/glass substrates using the procedure described earlier. A 250-nm mesoporous-TiO $_2$  layer was then deposited by spin-coating followed by a sintering heat-treatment of 500 °C for 30 min in air. A 1.5 wt % solution of SnCl $_4$  in distilled water was spin-coated at 3000 rpm for 30 s. This is followed by annealing at 200 °C for 30 min, forming an ultrathin compact SnO $_2$  layer. The addition of SnO $_2$  coating is for purpose of enhancing the overall device open-circuit voltage and does not have an obvious effect on the solution wetting. The thin films of MAPbI $_3$  modified with or without the MA $^+$ TFA $^-$  additive were then deposited according to the procedure described above. A solution of Spiro-MeOTAD (Merck Group, Germany) hole-transporting material (HTM) coating was prepared by dissolving 72.3 mg of Spiro-MeOTAD in 1 mL of chlorobenzene (99.8%), to which 28.8  $\mu\text{L}$  of 4-tert-butyl pyridine (96%) and 17.5  $\mu\text{L}$  of lithium bis(trifluoromethanesulfonyl)imide (LITSFI) solution (520 mg LITSFI in 1 mL acetonitrile) were added. The HTM was deposited by spin-coating (3000 rpm, 30 s). Finally, a 100 nm Au electrode was thermally-evaporated to complete the solar cells. The current density-voltage (J-V) of the solar cells were measured using a Keithley 2400 sourcemeter under simulated AM1.5 illumination (100 mW cm $^{-2}$ ) simulated using a solar simulator (Sol3A Class AAA, Oriol, USA). A non-reflective mask (0.09 cm $^2$ ) was used to define the PSC area. The stabilized maximum-power outputs of the PSCs were measured by monitoring the J outputs at the maximum-power V bias (deduced from the reverse-scan J-V curves). The external quantum efficiency (EQE) spectra were recorded with an EQE measurement system (Newport, USA).

## Supplementary Figures



**Figure S1.** Photograph of 70 wt% clear solution of MA<sup>+</sup>TFA<sup>-</sup> in DMF, demonstrating the high solubility.

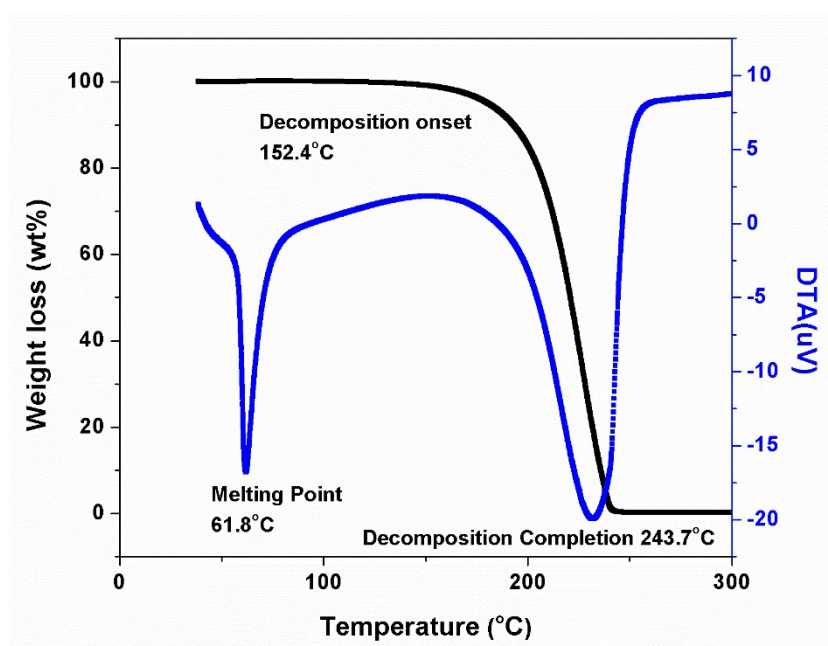


**Figure S2.** TG-DTA result of MA<sup>+</sup>TFA<sup>-</sup>, showing the melting point of 61.8 °C, and the decomposition onset at 152.4 °C and completion at 243.7 °C.

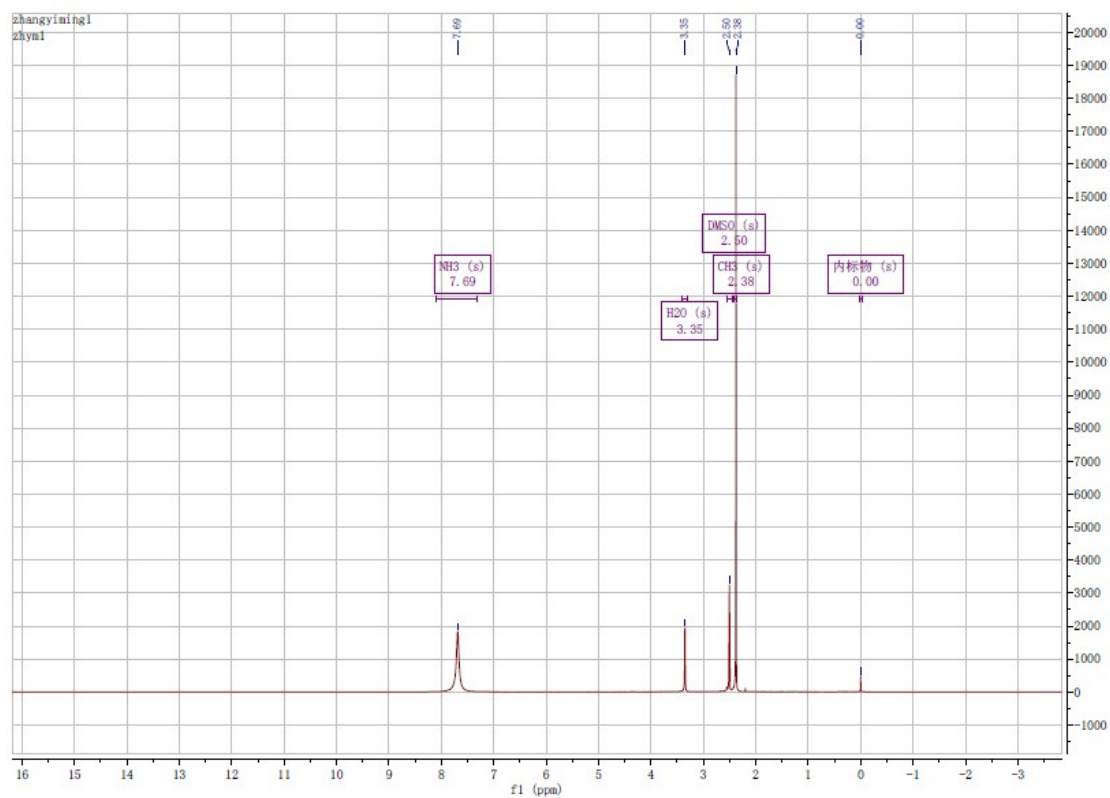


**Figure S3.** <sup>1</sup>H NMR spectrum (DMSO-d<sub>6</sub>, 400 MHz, TMS) of MA<sup>+</sup>TFA<sup>-</sup>.

<sup>1</sup>H NMR:  $\delta$  7.69 (s, 4H), 2.38 (s, 3H), demonstrating the existing of CH<sub>3</sub>NH<sub>3</sub><sup>+</sup> cation in DMSO.

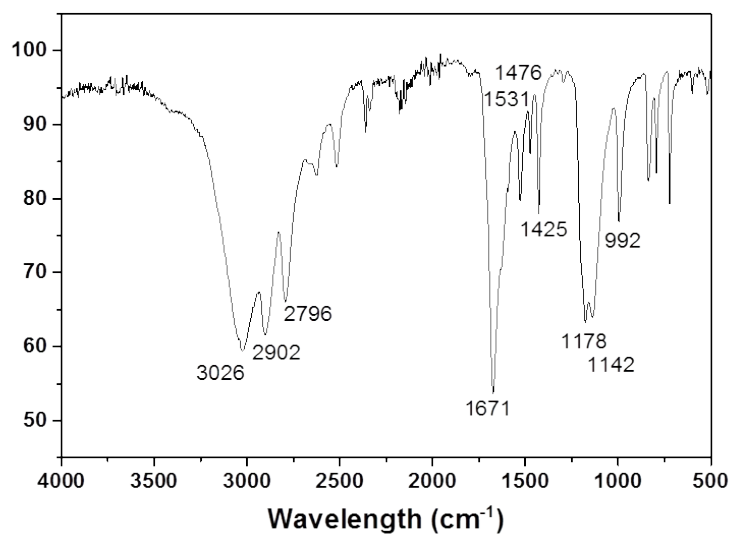


**Figure S4.** FTIR spectrum of MA<sup>+</sup>TFA<sup>-</sup>. The valleys are assigned as below: 3026 cm<sup>-1</sup> for  $\nu$  N-H, which confirms the existing of -NH<sub>3</sub>; 2902 cm<sup>-1</sup> for  $\nu^s$  C-H, 2796 cm<sup>-1</sup> for  $\nu^{as}$  C-H, 1476 cm<sup>-1</sup> for  $\delta^{as}$  C-H; 992 cm<sup>-1</sup> for  $\nu$  C-H, suggesting the existence of methyl group; 1425 cm<sup>-1</sup> for  $\delta^s$  C-H in -N-CH<sub>3</sub>, which confirms N atom is adjacent to methyl group, all above demonstrate the existence of CH<sub>3</sub>NH<sub>3</sub><sup>+</sup> cation. 1178 and 1142 cm<sup>-1</sup> for  $\nu$  C-F, 1671 cm<sup>-1</sup> for  $\nu$  C=O, 1531 cm<sup>-1</sup> for  $\nu$  C-O, all these prove the existing of the anion CF<sub>3</sub>COO<sup>-</sup>.

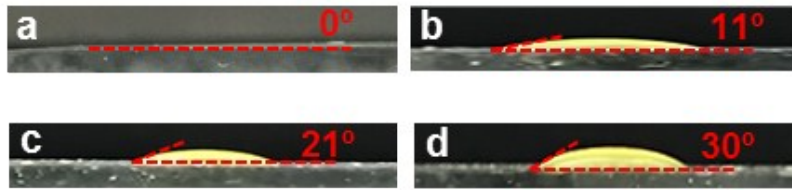


**Figure S5.** Cross-sectional optical images of MAPbI<sub>3</sub> perovskite solution droplets on compact-TiO<sub>2</sub>-coated FTO-glasses with the increasing weight ratio of MA<sup>+</sup>TFA<sup>-</sup> to MAPbI<sub>3</sub>: (a) 0; (b) 1:35; (c) 1:15, (d) 1:10.

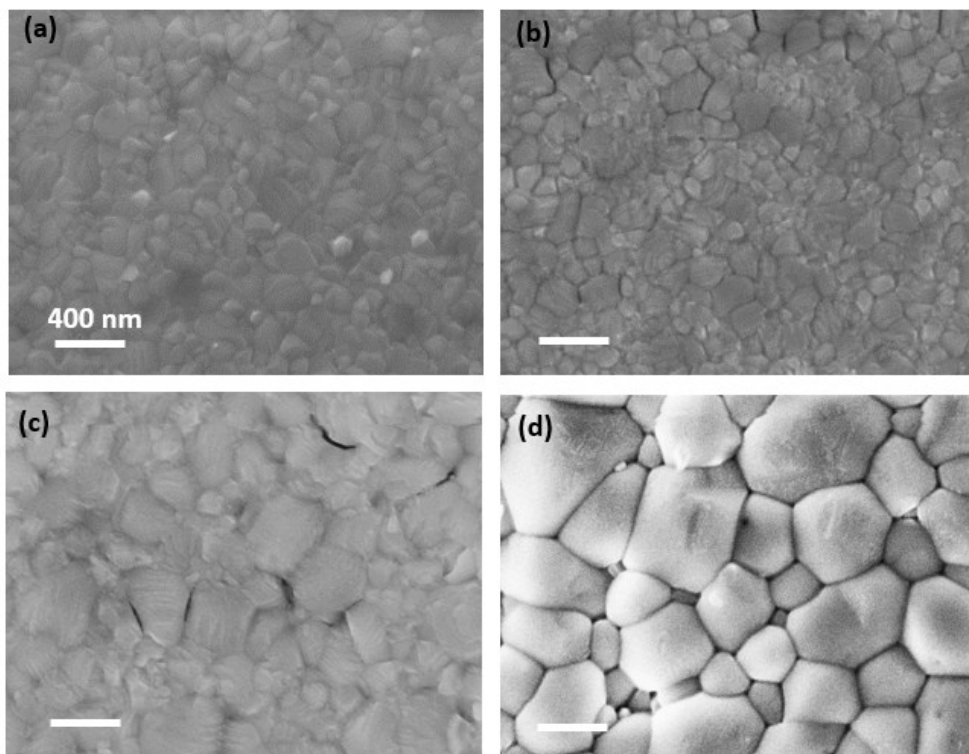


**Figure S6.** SEM images of MAPbI<sub>3</sub> perovskite thin films on compact-TiO<sub>2</sub>-coated FTO-glasses made with different weight ratios of MA<sup>+</sup>TFA<sup>-</sup> to MAPbI<sub>3</sub>: (a) 0; (b) 1:35; (c) 1:15; (d) 1:10. Note that (a) and (d) are reproduced from Figure 1c and 1d.



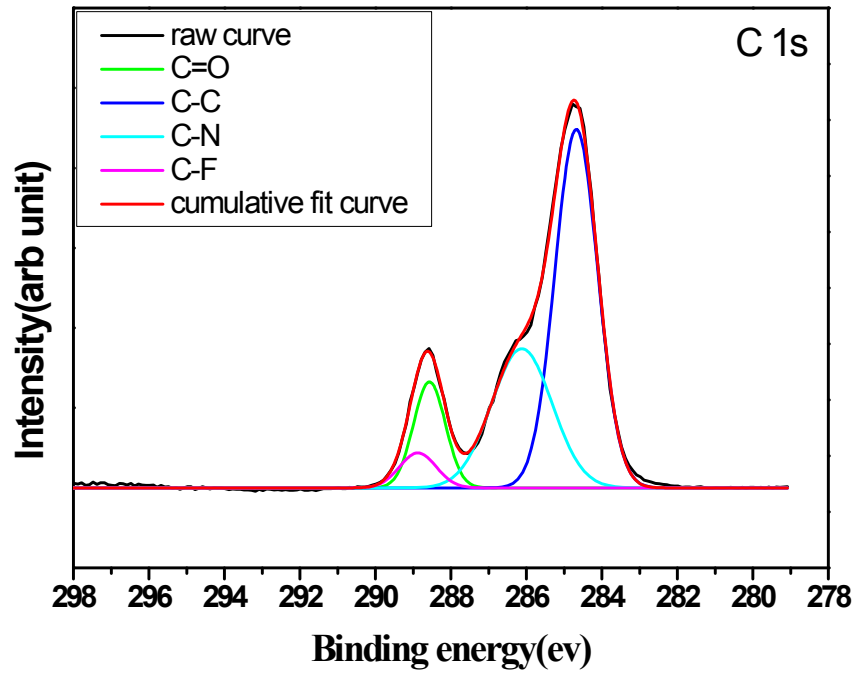


**Figure S7.** C 1s XPS of MAPbI<sub>3</sub> perovskite thin film made with MA<sup>+</sup>TFA<sup>-</sup>.

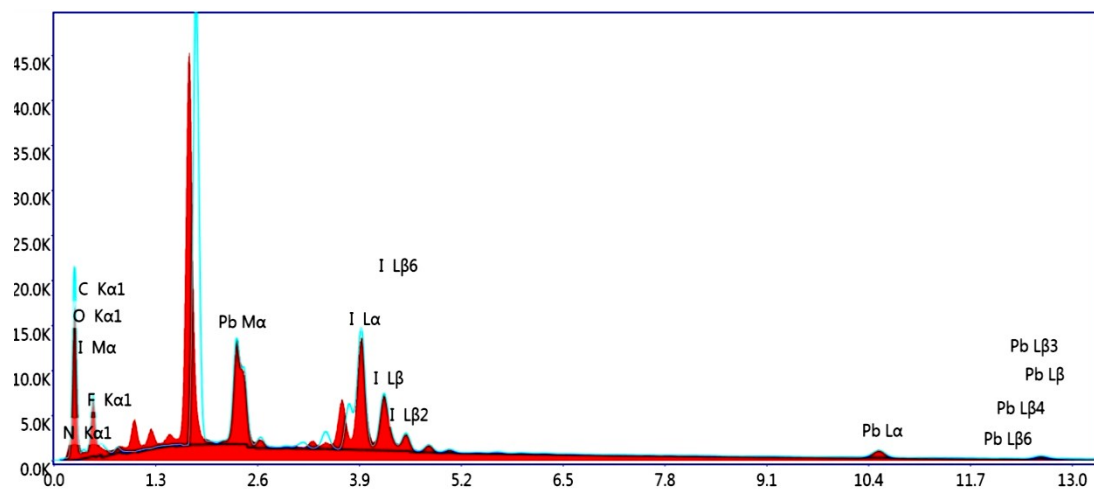


**Figure S8.** EDX spectrum of MAPbI<sub>3</sub> perovskite thin film made with MA<sup>+</sup>TFA<sup>-</sup>.

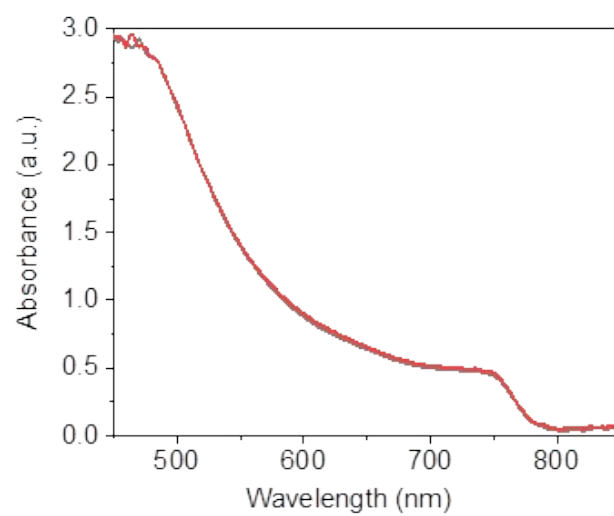


**Figure S9.** UV-vis absorption spectra of MAPbI<sub>3</sub> perovskite thin films made without (grey solid line) and with (red solid line) MA<sup>+</sup>TFA<sup>-</sup> additive.

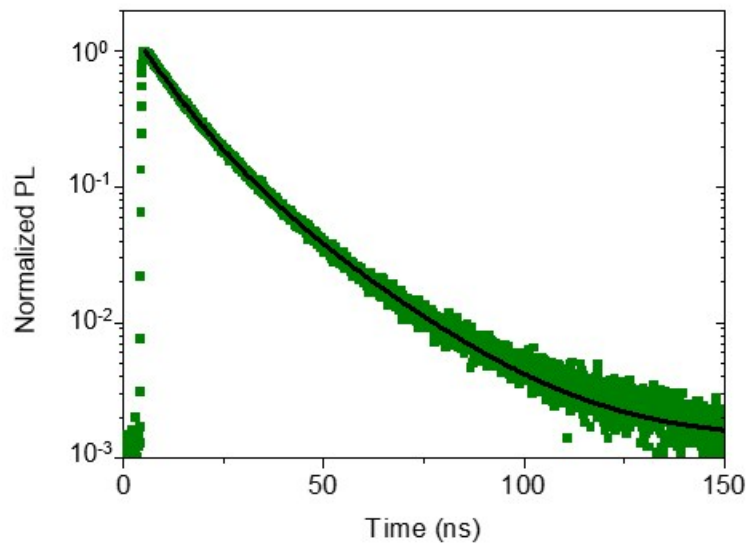
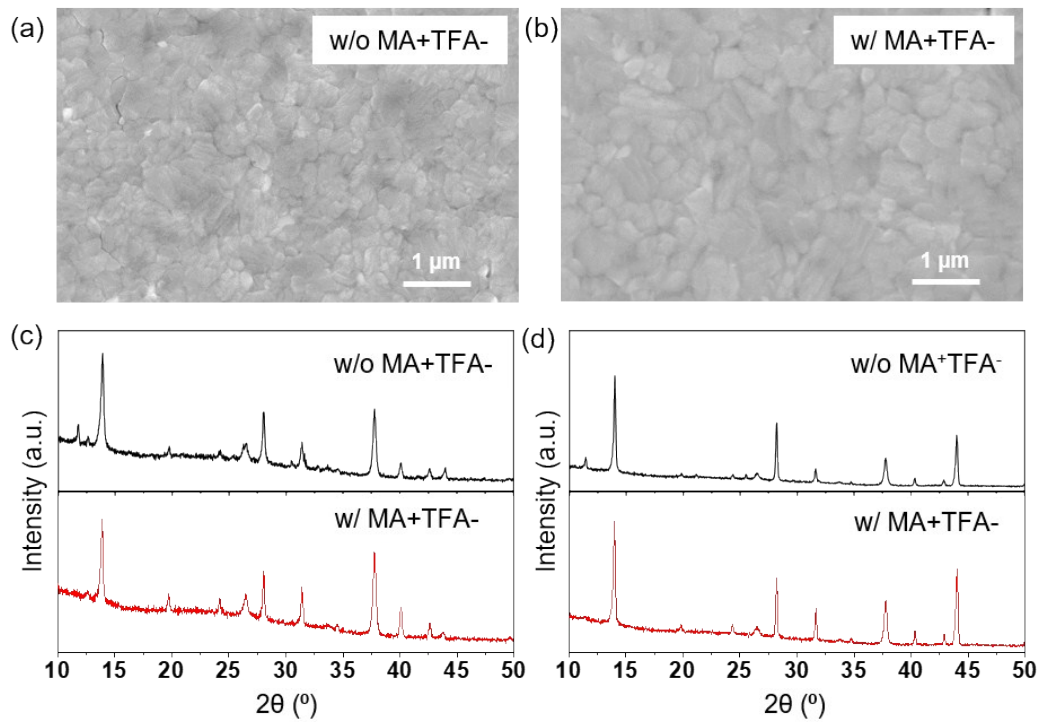


**Figure S10.** Time-resolved PL spectrum of the MAPbI<sub>3</sub> perovskite thin film that is made using solvent annealing method [ref: doi:10.1002/adma.201401685] and exhibit a similar grain size to the film made with MA<sup>+</sup>TFA<sup>-</sup> additive in this study. The spectrum is fit using a bi-exponential function and the fitting parameters are included in Table S1.



**Fig**

**Figure S11.** SEM images of the FAPbI<sub>3</sub> perovskite thin film made (a) without and (b) with MA<sup>+</sup>TFA<sup>-</sup> additive. (c) XRD patterns of the FAPbI<sub>3</sub> perovskite thin film made without and with MA<sup>+</sup>TFA<sup>-</sup> additive after storage 48-h exposure to the controlled humid condition (70% RH, RT). (d) XRD patterns of the MA<sub>0.7</sub>FA<sub>0.3</sub>PbI<sub>3</sub> perovskite thin film made without and with MA<sup>+</sup>TFA<sup>-</sup> additive after storage 48-h exposure to the controlled humid condition (70% RH, RT).

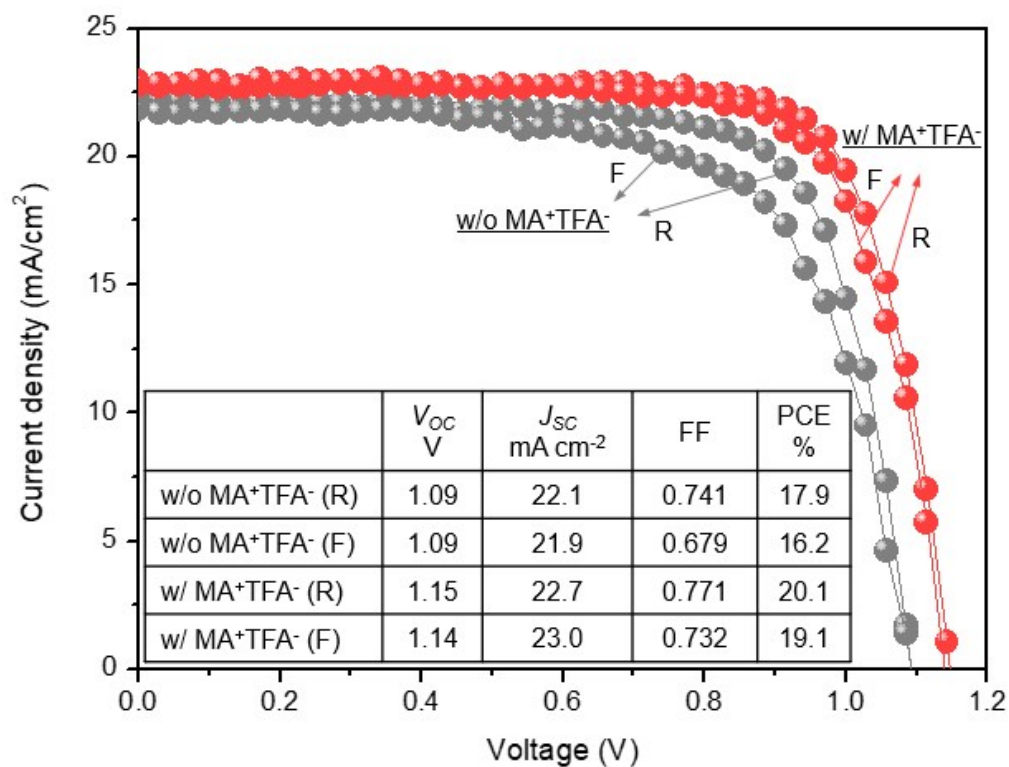


**Figure S12.** J-V curves at both forward (F) and reverse (R) scans for the best PSCs made without and with MA<sup>+</sup>TFA<sup>-</sup> additive. Inset shows the extracted J-V parameters.

**Table S1.** Time constants for fitting the PL decays in Figure 3b using bi-exponential functions.  $\tau_{\text{avg}}$  is the amplitude average PL lifetime.

	$\tau_1$	$\tau_2$	$\tau_{\text{avg}}$
w/ MA <sup>+</sup> TFA <sup>-</sup>	10.9 ns	20.6 ns	15.6 ns
w/o MA <sup>+</sup> TFA <sup>-</sup>	6.1 ns	24.0 ns	6.3 ns
w/ MA <sup>+</sup> TFA <sup>-</sup> (solvent-annealed)	8.8 ns	20.5 ns	12.2 ns